

# Improved Continuum Skin and Proximity Effect Model for Hexagonally Packed Wires

D. C. Meeker

*QinetiQ North America, 350 Second Ave., Waltham, MA 02451*

---

## Abstract

This work presents approximate but closed-form expressions for “effective” complex-valued magnetic permeability and electric conductivity that represent the effects of proximity and skin effect losses in wound coil with hexagonally packed wires. Previous work is extended by providing improved accuracy versus finite element results for effective permeability and by providing an expression for effective conductivity, which was previously neglected. These material properties can then be used in 2D/axisymmetric finite element models in which the coil is modeled as a coarsely meshed, homogeneous region (*i.e.* removing the need for modeling each turn in the coil).

*Keywords:* Eddy currents, skin effect, proximity effect, homogenization

---

## 1. Introduction

Continuum representations of skin/proximity effect losses in wound coils suitable for inclusion in 2D/axisymmetric finite element analyses have been previously reported in the literature. Moreau *et al.* [1] described the use of a complex-valued magnetic permeability for the continuum representation of transformer windings with rectangular conductors, presenting closed-form expressions for frequency-dependent permeability. Podoltsev *et al.* [2] consider windings with round wires assuming that the turns are packed in a square grid. Numerical solutions for complex-valued permeability for different fills are presented graphically. Gyselinck and Dular [3] present a numerical method for obtaining effective properties of a round-wire winding with hexagonal packing. Xi Nan and Sullivan [4] and Rossmanith *et al.* [5] present analytical formulas for proximity effect losses in hexagonal windings. Parameters in these analytical formulas are then tuned to match finite element proximity effect results. An extension of the model to a continuum representation of square-packed Litz wire bundles is also considered in [4]. However, formulas for skin effects are neglected in both works.

---

*Email address:* [dmeeker@ieee.org](mailto:dmeeker@ieee.org) (D. C. Meeker)

Previously, continuum representations were primarily used for the purposes of proximity effect computation during transformer design. However, the purpose of the present development is to obtain formulas that can be ubiquitously and automatically applied to wound regions in AC magnetic finite element analyses. The formulas are meant to be used on general wound regions like air-cored coils, slotless motors, magnetic bearings, and so on. One implication of the desire for a generally applicable representation is the focus on hexagonal packing. Although it is practically difficult to obtain a perfect hexagonal packing, wires in these devices tend to lay down in fashion that approaches a hexagonal fill. Therefore, the present work focuses exclusively on hexagonally packed windings. A second implication for the desire for a generally applicable formula is that the fit for both the real and imaginary parts of the permeability must be excellent. Some previous works (*e.g.* [4]) have focused on fitting to the imaginary part of the complex permeability because it is closely related to losses for a given field intensity. However, an accurate estimate of the real portion of the permeability is also needed to ensure that the right field intensity is computed in the winding in finite element domains with more general arrangements.

Similar to previous works, this work provides an analytical form for effective permeability with parameters fit to finite element results. However, the present work extends the previous efforts in several ways:

- The present work provides an expression for effective conductivity that is a good fit to finite element results. Expressions for effective conductivity (related to skin effect) are neglected in previous works with hexagonal packing.
- The combination of the analytical form and selected parameters for effective permeability (related to proximity effect) presented in the present work provides a more accurate fit to finite element results than previously published results.
- The parameters in functional forms from previous works are revisited using a broader set of finite element results and a different cost function for parameter selection. “Re-tuned” parameters for the previous works are presented that improve the performance of those approaches.

## 2. Finite Element Calculations of Effective Properties

Previous work considered a purely analytical expression for proximity and skin effect losses based on an equivalent foil approach.[6] The foil geometry is an essentially 1-D problem in which it is straightforward to split the problem in to separate analyses that address proximity effect, skin effect, and flux linkage. In case of square wires, (*e.g.* as addressed in [7]), it is straightforward to pick boundary conditions that address the skin and proximity effect problems for a column of wires. However, for a hexagonally packed column of wires, as shown in Figure 1, there is no obvious edge to which the boundary conditions can be applied. Instead, a 2-D domain must be defined that can be broken down into

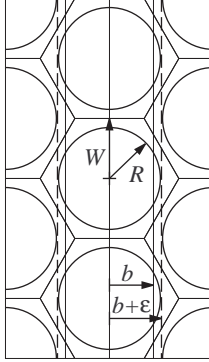


Figure 1: Hexagonally packed winding and equivalent foil geometry.

analogous proximity and skin effect problems. That geometry, along with the proximity and skin effect sub-problems is shown in Figure 2.

### 2.1. Skin Effect Computation

Like in [7], to obtain a result relevant to skin effect computation, a domain with odd symmetry from between columns of wires is needed. For the case of foil conductors like in [6], this condition can be imposed by explicitly applying vector potential  $A = 0$  in on a line bisecting the gap between conductors. However, the same boundary condition could have been implicitly imposed by an infinite array of foils carrying alternating current directions. Since there is no one line on which to apply  $A = 0$  in the hexagonal case, the geometry of Figure 2b applies an approach similar to method of images, creating a geometry with alternating rows of wire carrying alternating current directions. The condition  $A = 0$  is defined only at only point in the center of the domain, and  $dA/dn = 0$  boundary conditions are defined on all edges.

This solution is used to obtain  $\rho_r$ , a frequency-dependent resistivity of the wire in the finite element solution domain. A commonly available finite element post-processing result is the complex impedance,  $Z$ , of the series-connected circuit used to drive the currents in the problem domain. Some care must be taken, depending upon exactly how the problem is step up. If one circuit is defined to drive both the positive and negative current, the length of the circuit is twice the length of the solution in the into-the-page direction, but the cross-section area of the circuit is only 1/2 of the solution domain. Therefore,  $\rho_r$  can be obtained from the FEA-derived impedance via:

$$\rho_r = \left( \frac{\sqrt{3}W^2}{4L} \right) Z \quad (1)$$

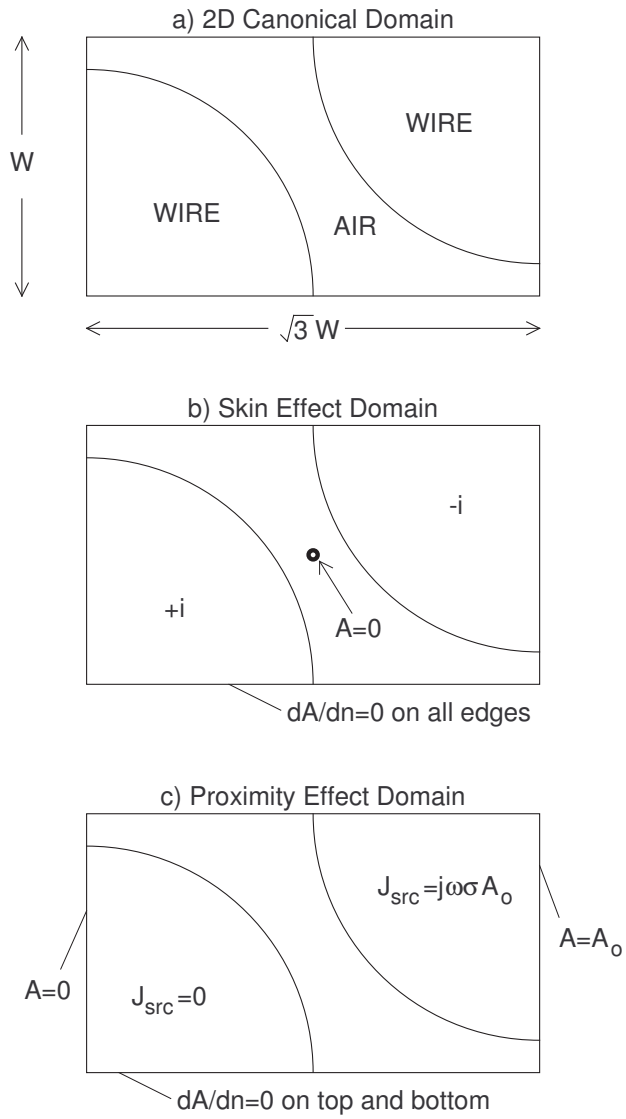


Figure 2: Solution domain for hexagonal proximity and skin effect computation.

## 2.2. Proximity Effect Computation

Similarly, as in [7], to obtain a result relevant to proximity effect computation, a domain with even symmetry is required. For the case of foil conductors, like in [6], it is straightforward to pick Dirichlet boundary condition the lines at the center of the gaps between foils that enforces even symmetry (and assures that no net current is carried by the foil). However, in the case of hexagonally packed conductors, there isn't one line between columns of wires along which a Dirichlet boundary condition can be applied.

However, it can be noted that the line that goes down the center of each row of wires is an isocline of  $A$  in the proximity effect problem. To ease the definition of boundary conditions in the hexagonally packed case, it is better to take advantage of this line of constant  $A$ , drawing the domain as pictured in Figure 2c. It is convenient to define the left edge of the domain as  $A = 0$ . The right side of the domain is then set to an arbitrary potential,  $A_o$ .

The proximity problem is meant to address the case in which there is no net current in any of the wire, just circulating currents that are conserved within the cross-section of each wire. The voltage gradient on each conductor due to the applied boundary conditions is:

$$\Delta v = -j\omega A_{ctr} \quad (2)$$

where  $A_{ctr}$  is the potential at the the center of the conductor in question. To force the wires to carry a zero net current, a source current density of

$$\Delta v = j\omega\sigma A_{ctr} \quad (3)$$

must be imposed to cancel out the induced current, *i.e.* to model an open-circuit condition.

This domain is used to determine an effective permeability including proximity effects. Two common FEA post-processing calculations are time averaged stored energy per unit volume (here represented as  $w$ ), and time averaged losses ( $p$ ), both taken over the entire solution domain. If the domain were, instead, composed of a homogeneous material, the stored energy and loss densities would be:

$$w = \frac{1}{4} \frac{\mu_r}{|\mu|^2} \bar{B}^2 \quad (4)$$

$$p = -\frac{\omega}{2} \frac{\mu_i}{|\mu|^2} \bar{B}^2 \quad (5)$$

where

$$\mu_{eff} = \mu_r + j\mu_i \quad (6)$$

Using (4) and (5), it is straightforward to obtain the  $\mu_{eff}$  of an equivalent homogeneous material:

$$\mu_{eff} = \frac{\omega \bar{B}^2}{2jp + 4\omega w} \quad (7)$$

### 3. Approximating Function

Although the techniques in Section 2 would alone be a suitable method for determining the equivalent properties for any region, it is desirable to have a closed-form approximating function that can represent the results obtained from a large set of finite element runs. To aid in forming an approximation function, it is useful to present the non-dimension frequency,  $\Omega$ :

$$\Omega = \left( \frac{\sigma \mu_o R^2}{2} \right) \omega \quad (8)$$

This non-dimensionalization is selected so that  $\Omega = 1$  coinciding with the frequency at which the skin depth is the same as the wire radius,  $R$ .

To represent the numerical results, it is assumed that forms similar to the expressions derived from an equivalent foil approach in [6] will be sufficient. The forms that are proposed are:

$$\mu_{eff} = (1 - c_2)\mu_o + c_2\mu_o \frac{\tanh \sqrt{j c_1 \Omega}}{\sqrt{j c_1 \Omega}} \quad (9)$$

$$\rho_r = \left( \frac{1}{\sigma \text{ fill}} \right) \left( \frac{\sqrt{j c_3 \Omega}}{\tanh \sqrt{j c_3 \Omega}} + j c_4 \Omega \right) \quad (10)$$

The effective properties of the gapped foil region for use in an equivalent continuum model are permeability  $\mu_{eff}$  prescribed by (9) and conductivity described by (11):

$$\sigma_{eff} = \frac{1}{\rho_r - \frac{1}{3} j \omega \mu_{eff} (b + \epsilon)^2} \quad (11)$$

where  $c_1, c_2, c_3$  and  $c_4$  are to-be-determined functions of copper fill factor (denoted as “fill”). The  $(b + \epsilon)$  term represents  $1/2$  the wire row pitch, as pictured in Figure 1.

To define some of the unknown parameters, it is desirable to select  $c_1$  through  $c_2$  to enforce low-frequency asymptotic proximity losses exactly (*e.g.* as had been previously done in [7]). In the low frequency limit where the reaction field of the induced currents can be neglected, the proximity losses can be written exactly as (see Appendix A):

$$\mu_{eff}|_{\Omega \rightarrow 0} = \mu_o \left( 1 - \frac{1}{2} j \text{fill} \Omega \right) \quad (12)$$

The Taylor series of (9) about  $\Omega = 0$  is:

$$\mu_{eff} \approx \mu_o \left( 1 - \frac{1}{3} j c_1 c_2 \Omega \right) \quad (13)$$

The asymptotic losses are satisfied exactly if:

$$c_2 = \frac{3 \text{ fill}}{2 c_1} \quad (14)$$

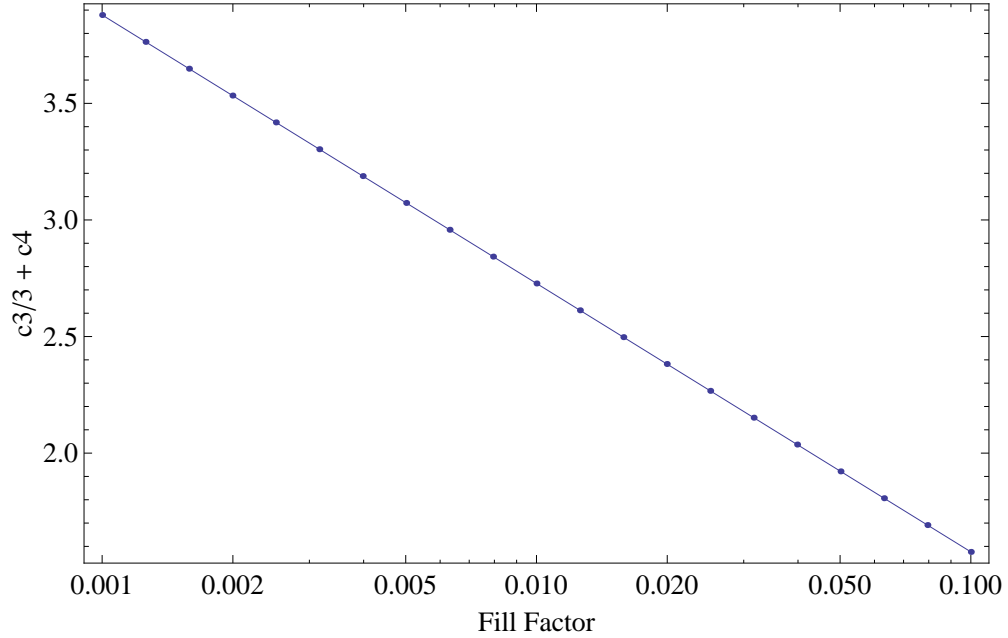


Figure 3: Relationship of Skin Effect Parameters at Low Fill Factor.

Similarly,  $c_3$  through  $c_4$  can be selected to enforce the asymptotic behavior of  $\rho_r$  for small fill factors. The Taylor expansion of (10) about  $\Omega = 0$  is:

$$\rho_r \approx \frac{1}{\sigma \text{ fill}} \left( 1 + \frac{j}{3}(c_3 + 3c_4)\Omega \right) \quad (15)$$

Unlike the proximity effect problem, a closed-form asymptotic solution is not clear. The quantity  $\rho_r$  was evaluated at  $\Omega = 0.01$  over a range of fills from 0.001 to 0.1 at 31 points evenly distributed on a log scale. The evaluations of  $\rho_r$  can then be processed as implied by (10) to obtain finite element estimates of the quantity  $\frac{1}{3}c_3 + c_4$ :

$$\frac{1}{3}c_3 + c_4 = \text{fill} \text{Im}\left(\frac{\rho_r \sigma}{\Omega}\right) \quad (16)$$

As shown in Figure 3, the finite element results are well fit by a curve that varies with the log of fill:

$$\frac{1}{3}c_3 + c_4 = 0.425218 - \frac{\log(\text{fill})}{2} \quad (17)$$

Now, expressions for  $c_1$  and  $c_3$  as a function of fill must be determined. It was assumed that both functions could be suitably approximated as cubic polynomials in fill. Both  $\rho_r$  and  $\mu_{eff}$  were evaluated at a large number of points. The functions were evaluated at fill factors between 0.1 and 0.9 at

increments of 0.1 and at 51 frequency points evenly distributed on a log scale between  $\Omega = 0.01$  and  $\Omega = 1000$ , 459 data points in all. Problems were solved with meshes containing on the order of 10,000 elements with the freely available FEMM finite element program [9].

Since  $\mu_{eff}$  and  $\rho_r$  have a fairly wide dynamic range, the normalized RMS error on between the analytical formula and the FEA results is a reasonable metric for comparing goodness of fit. For some complex-valued data set,  $z$ , and some approximation,  $\hat{z}$ , the normalized RMS error is defined as:

$$\text{Normalized RMS Error} = \left[ \sum_1^n \frac{1}{n} \left| \frac{z_n - \hat{z}_n}{z_n} \right|^2 \right]^{\frac{1}{2}} \quad (18)$$

The parameters of the polynomials describing  $c_1$  and  $c_3$  were selected to minimize this cost function. For the  $\mu_{eff}/\mu_o$ , as plotted in Figure 4, the RMS error is 1.23%. For the  $1/(\sigma\rho_r)$  quantity plotted in Figure 5, the RMS error is 2.35%. The forms of  $c_1$  and  $c_2$  that minimize (18) are:

$$c_1 = -0.0714373 \text{ fill}^3 + 0.0684158 \text{ fill}^2 + 0.687385 \text{ fill} + 0.775607 \quad (19)$$

$$c_3 = -0.215718 \text{ fill}^3 + 0.722321 \text{ fill}^2 - 0.00860551 \text{ fill} + 0.882464 \quad (20)$$

The finite element results are plotted along with the approximating function in Figure 4 for  $\mu_{eff}$  and in Figure 5 for  $\rho_r$ .

#### 4. Comparisons to Previous Results

First, the performance of the Rossmannith formula [5] was evaluated. It was found to have be an excellent match to finite element data at relatively low frequency, in the region where  $\Omega < 10$ . However, for higher values of  $\Omega$ , the fit diverges from the finite element results. However, the parameters in [5] appear to be fit from a relatively small number of runs and over a smaller range of  $\Omega$  than considered in the present work. To provide a fair comparison of results, the parameters in the model were re-fit using the the same finite element data set and cost function (18) used to obtain the parameters for the present model. The curve fit permeability equation obtained in is plotted in Figure 6 along with the finite element results used for curve fitting in this work. With the returned parameters, the match to finite element data is substantially improved, providing a relatively in amplitude to finite element data over a wide range of frequencies. Agreement of the imaginary portion of the complex permeability shows some erratic behavior at higher frequencies.

$$\begin{aligned} v &= 1 - 1.56856k + 0.602779k^2 \\ w_z &= \left[ 1.30413 + \frac{7.05284}{z^2} - \frac{0.305487z^2}{z^2 + 297.931(1+i)} \right]^{-1} \end{aligned} \quad (21)$$

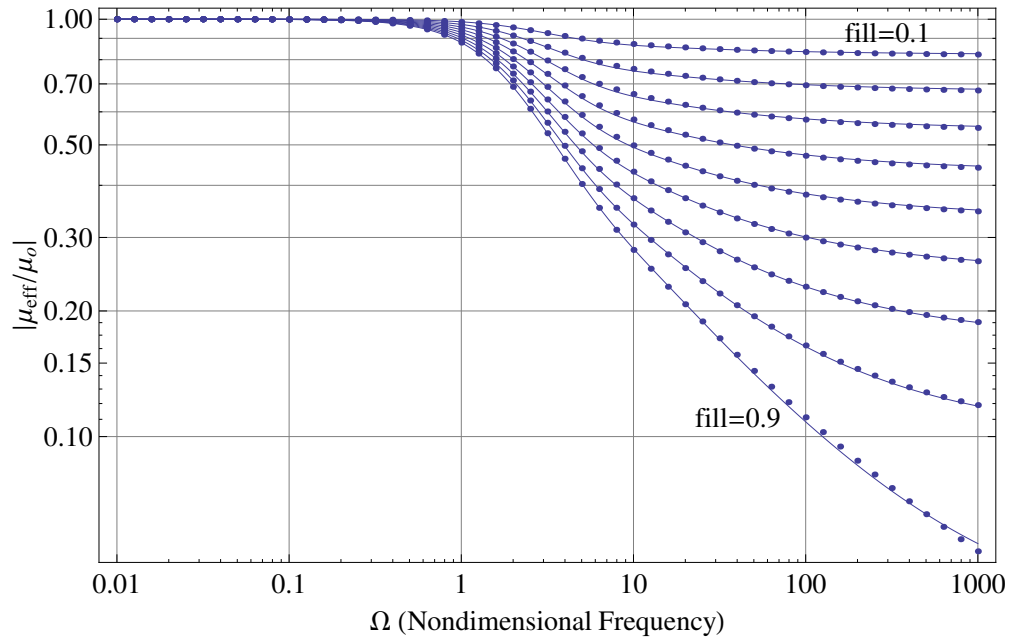
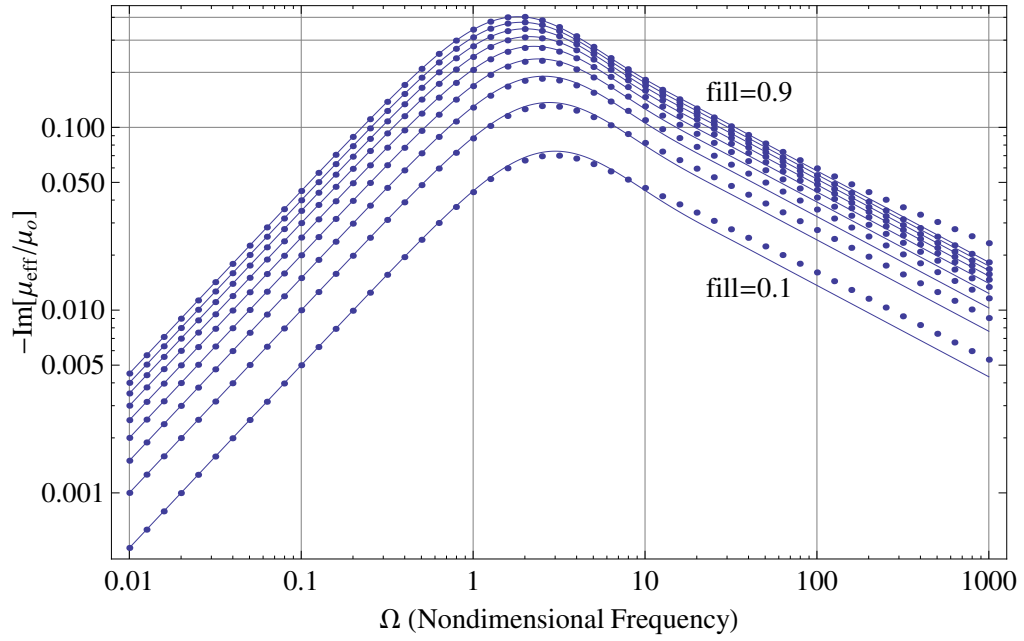


Figure 4: Proximity finite element results and approximating function for fill from 0.1 to 0.9

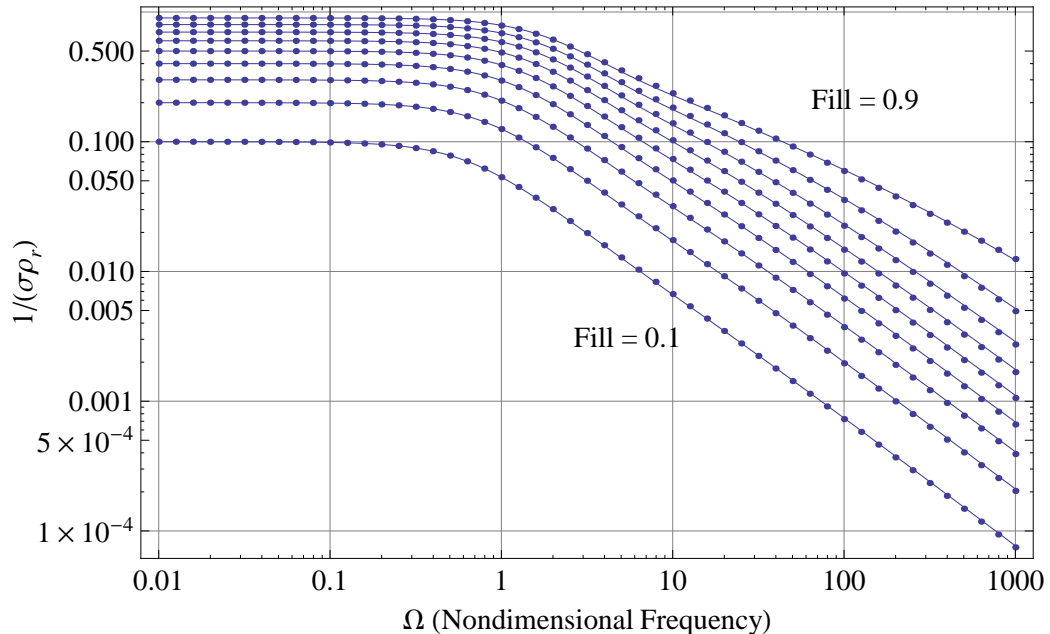


Figure 5: Skin effect finite element results and approximating function for fill from 0.1 to 0.9

Finite element results were then compared with the form and fitting parameters in [4]. It was found that the form for the imaginary part of complex permeability in [4] must be multiplied by a factor of 2 to adjust for an apparent Peak vs. RMS scaling error. With the fitting parameters as presented in [4], the fit of the imaginary part of the permeability in [4] to finite element results is good at low frequencies and good at high frequencies, especially for low fills. However, there are errors in the imaginary part of permeability the range of 10%-25% in the transition region between the low and high frequency regimes. With the original parameters, the fit to the amplitude of the permeability is poor (greater than 30% RMS error).

However, much better performance can be obtained with the [4] formulation by retuning the parameters. In the original work, the parameters were fit to the imaginary portion of permeability only. The use of (18) tends to find a good fit to both real and imaginary parts of the permeability. Optimized re-tuned parameters, using the nomenclature of [4], are given in (22). Plots of the fit are shown in Figure 7.

$$\begin{aligned}
 k_{hex} &= 0.81419 - 0.0851379\lambda \\
 b_{hex} &= 0.250995 + 0.29522 \exp(-6.31359\lambda) \\
 w_{hex} &= 0.113135
 \end{aligned} \tag{22}$$

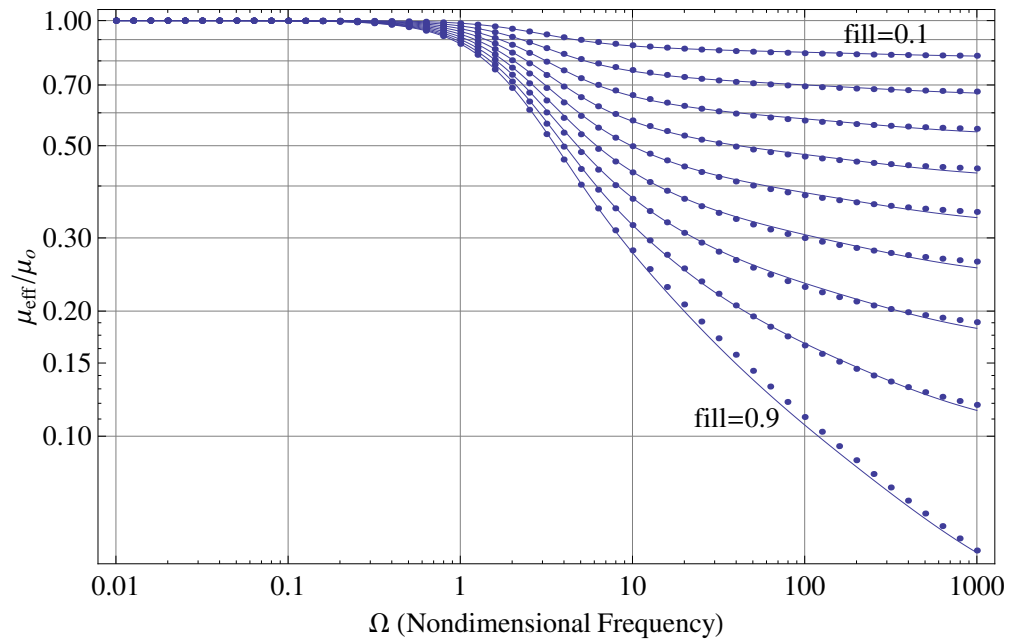
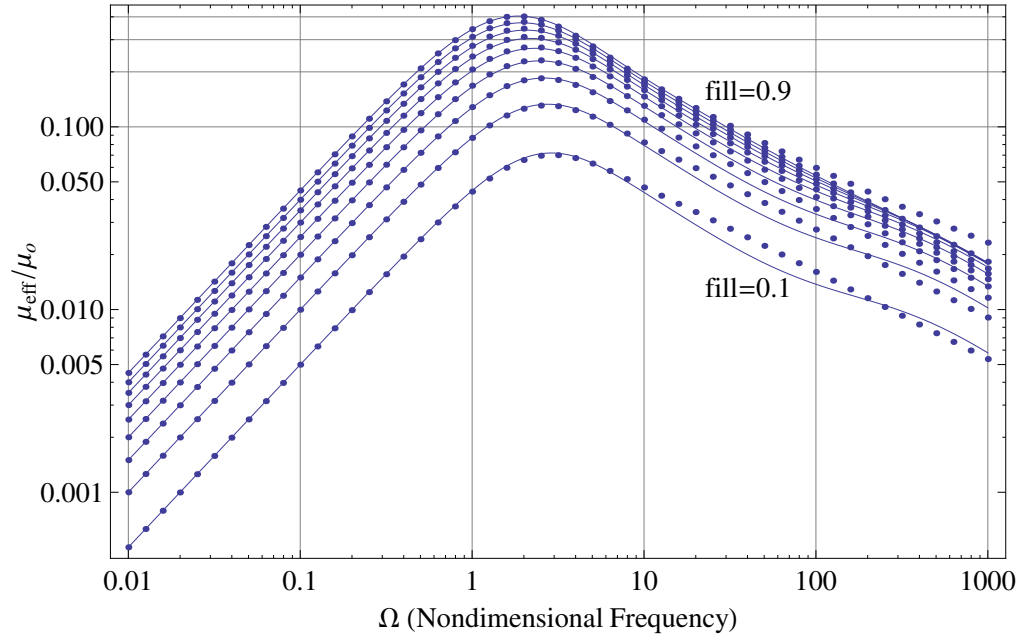


Figure 6: Re-tuned Rossmannith [5] complex permeability vs. finite element results.

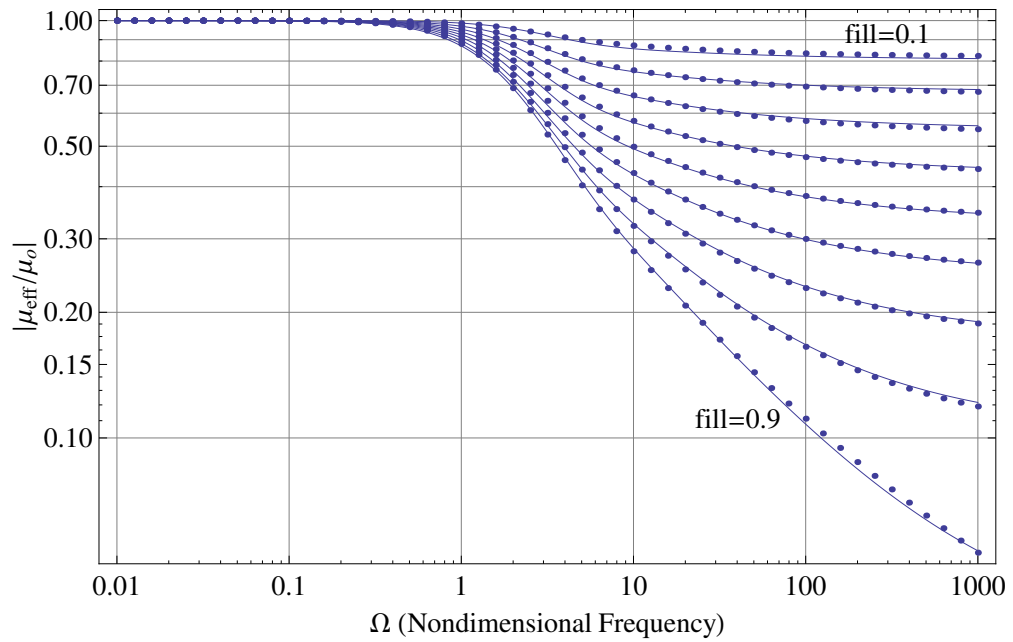
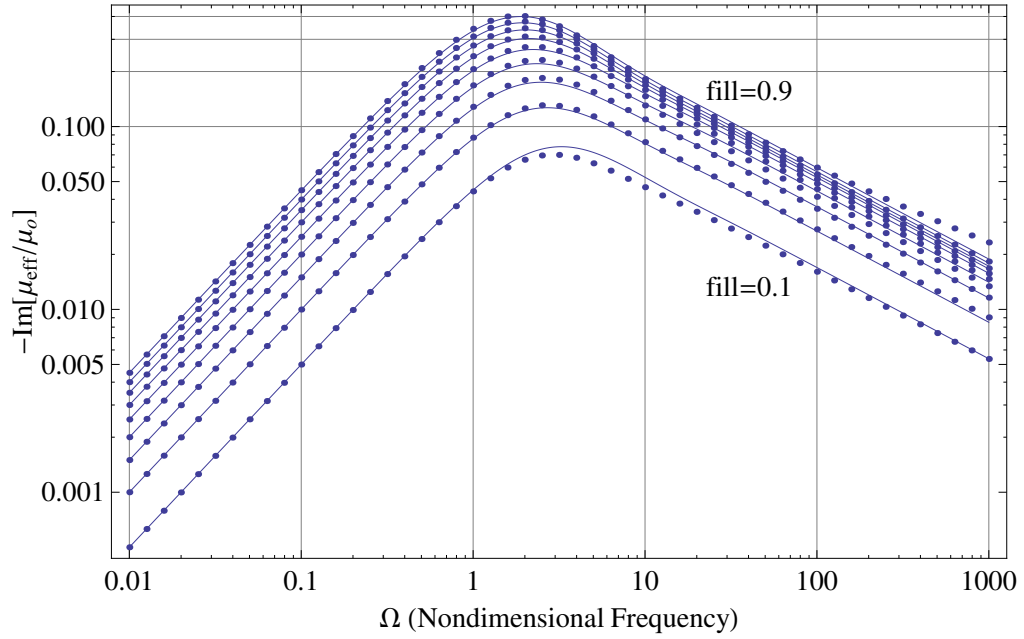


Figure 7: Re-tuned [4] complex permeability vs. finite element results.

Model	[4] Orig	[4] Re-tune	[5]	[5] Re-tune	Present
$ \mu $	21.2%	1.41%	8.72%	1.62%	1.23%
$\text{Im}[\mu]$	6.15%	4.23%	32.1%	4.70%	5.13%

Table 1: Normalized error comparison of various fitting models.

The various models can be quantitatively compared via the normalized RMS error used as a parameter-fitting cost function in (18). The normalized RMS error was computed as directly in (18) and, for reference purposes, considering only the imaginary part of the complex permeability. The results are shown in Table 4. The approach of the present work has a better overall agreement to finite element-derived complex permeability than previously published approaches. Performance is about the same as the re-tuned version both alternative formulas.

## 5. Conclusions

Equations (9) and (10) are closed-form approximations for equivalent continuum material properties for a region filled with hexagonally packed wires. The expressions are a significantly better match to finite element results than equations presented in previous works. However, part of the improvement over previous work is due to the parameters selected for the functional forms used in previous works. When the functional forms from previous works are re-tuned using the present data set and cost function, the gains over previously presented forms is more modest.

However, fitting of the imaginary part of the complex permeability is still not perfect at high frequency for very high fill factor for either the presently presented form or for previous works. Creation of a more elaborate model with better fit in these regions could be the subject of future work.

- [1] O. Moreau, L. Popiel, J. L. Pages, Proximity losses computation with a 2D complex permeability modelling, *IEEE Trans. Magn.* 34(1998) 3616-3619.
- [2] A. D. Podoltsev, I. N. Kucheryavaya, B. B. Lebedev, Analysis of effective resistance and eddy-current losses in multiterm winding of high-frequency magnetic components, *IEEE Trans. Magn.* 39(2003) 539-548.
- [3] J. Gyselinck, P. Dular, Frequency-domain homogenization of bundles of wires in 2-D magnetodynamic FE calculations, *IEEE Trans. Magn.* 41(2005) 1416-1419.
- [4] Xi Nan, C. Sullivan, An equivalent complex permeability model for litz-wire windings, *IEEE Ind. Appl. Soc. Ann. Meeting* (2005) 2229-2235.
- [5] H., Rossmanith, M. Albach, J. Patz, A. Stadler, Improved characterization of the magnetic properties of hexagonally packed wires, *Proc. Euro. Conf. on Power Electronics and Applications* (2011), 1-9.

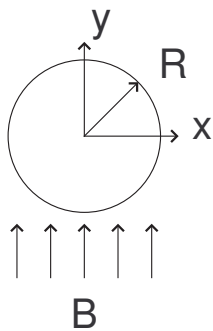


Figure A.8: Isolated wire in a magnetic field

- [6] D. C. Meeker, Effective material properties of wound coils from an equivalent foil approach, <http://www.femm.info/examples/prox/notes.pdf>.
- [7] Xi Nan, C. Sullivan, Simplified high-accuracy calculation of eddy-current losses in round-wire windings, IEEE Power Electronics Specialists Conf., (2004) 873879.
- [8] R. K. Erickson, Fundamentals of Power Electronics, Chapman and Hall, 1997.
- [9] D. C. Meeker, Finite Element Method Magnetics, Version 4.2 (09Nov2010 Build), <http://www.femm.info>
- [10] R. Sabariego, P. Dular, J. Gyselinck, Time-domain homogenization of windings in 3-D finite element models, IEEE Trans. Magn. 44(2008):1302-1305.

### Appendix A. Low Frequency Proximity Losses

Consider an isolated wire of radius  $R$  and conductivity  $\sigma$  as frequency  $\omega \rightarrow 0$  with no net current. The wire is immersed a time-varying magnetic field of amplitude  $B$  and frequency  $\omega$ . The eddy currents induced in the wire are governed by Faraday's law:

$$\frac{1}{\sigma} \nabla \times J = -j\omega B \tag{A.1}$$

Referring to Figure A.8, if the frequency low enough the the reaction field from the induced currents in the wire is negligible, the eddy currents in the wire can be obtained by directly integrating (A.1):

$$J = -j\omega\sigma Bx \tag{A.2}$$

The total proximity effect loss per unit length can be obtained by integrating the resistive losses over the wire's cross-section, assuming a Peak rather than an RMS scaling for all relevant quantities:

$$\begin{aligned} \text{loss} &= \frac{1}{2\sigma} \int_{-R}^R \int_{-\sqrt{R^2-x^2}}^{\sqrt{R^2-x^2}} |J|^2 dy dx \\ &= \frac{\pi}{8} \sigma \omega^2 B^2 R^4 \end{aligned} \tag{A.3}$$

$$= \frac{\pi}{8} \sigma (\mu_o \omega H)^2 R^4 \tag{A.4}$$

The complete area of the cell associated with the wire can be defined in terms of the wire's and fill factor as:

$$a_{\text{cell}} = \frac{\pi R^2}{\text{fill}} \tag{A.5}$$

so that the average loss per unit volume,  $p$ , can be written as:

$$p = \frac{\sigma_{\text{fill}}}{8} (\mu_o \omega R H)^2 \tag{A.6}$$

Recalling (5) and writing it in terms of  $H$ , rather than  $B$ :

$$p = -\frac{\omega}{2} \mu_i H^2 \tag{A.7}$$

Setting (A.6) equal to (A.7) and solving for  $\mu_i$  yields:

$$\mu_i = -\frac{1}{4} \text{fill} \omega \sigma \mu_o^2 R^2 = -\frac{1}{2} \mu_o \text{fill} \Omega \tag{A.8}$$

The low frequency effective permeability of the region, which accounts for proximity effect losses in the wire, is then:

$$\mu_{\text{eff}} \approx \mu_o \left( 1 - \frac{1}{2} j \text{fill} \Omega \right) \tag{A.9}$$